

CONDITIONS FOR CSR MICROBUNCHING GAIN SUPPRESSION*

C. -Y. Tsai[#], Department of Physics, Virginia Tech, VA 24061, USA
 D. Douglas, R. Li, and C. Tennant, Jefferson Lab, Newport News, VA 23606, USA
 S. Di Mitri, Elettra-Sincrotrone Trieste, 34149 Basovizza, Trieste, Italy

Abstract

The coherent synchrotron radiation (CSR) of a high brightness electron beam traversing a series of dipoles, such as transport arcs, may result in phase space degradation. On one hand, the CSR can perturb electron transverse motion in dispersive regions along the beamline, causing emittance growth. On the other hand, the CSR effect on the longitudinal beam dynamics could result in microbunching instability (MBI). For transport arcs, several schemes have been proposed to suppress the CSR-induced emittance growth. Correspondingly, several scenarios have been introduced to suppress CSR-induced microbunching gain, which however mostly aim for linac-based machines. In this paper we try to provide sufficient conditions for suppression of CSR-induced microbunching gain along a transport arc. Several example lattices are presented, with the relevant microbunching analyses carried out by our semi-analytical Vlasov solver [1]. The simulation results show that lattices satisfying the proposed conditions indeed have microbunching gain suppressed. We expect this analysis can shed light on lattice design approach that could control the CSR-induced microbunching gain.

OVERVIEW OF SUPPRESSION SCHEMES

For CSR-induced Emittance Growth

There have been many approaches proposed to minimize or cancel the CSR-induced emittance growth [2-9]. For example, Hajima [3] used the beam envelope matching method by characterizing the transverse phase-space ellipse tilt due to CSR. Jing *et al.* [5] studied a similar concept for ERL-based FEL in eRHIC. Douglas [2, 7] and Di Mitri *et al.* [4] employed cell-to-cell phase matching to compensate or cancel the CSR kicks. Jiao *et al.* [8] extended the above two methods to give generic conditions for suppression of the CSR-induced emittance growth in a two-dipole achromatic unit.

For CSR-induced Gain Amplification

The cure of MBI [10-14] can be undertaken either by enhancing Landau damping against microbunching amplification mechanism or by dedicated beamline designs. For the former, an effective way is to increase the uncorrelated energy spread [10,12-14]. As for the latter, the strategy of the beamline designs can be further categorized into two types: one is to make the relative momentum compaction function as small as possible

throughout the beamline; the other is to enhance the Landau damping via phase mixing (see, for more detail, Ref. [15]).

SUPPRESSION CONDITIONS BASED ON LINEAR OPTICS ANALYSIS

Our previous work [16] has indicated the important role of the relative momentum compaction for CSR microbunching gain development. Here we try to relate this important quantity to Twiss parameters. The following analysis is based on the numerical observation [16] that CSR microbunching development always originates from interactions between two dipoles (first stage) and can then accumulate over along the beamline (higher stages). Below we consider the simplest case for CSR interaction: dipole-achromat/straight-dipole module (see Fig. 1). The linear transport matrix from the emission site (s_i) to receiving site (s_f) can be obtained

$$\mathbf{R}_{6 \times 6}^{s_i \rightarrow s_f} = \mathbf{R}_{6 \times 6}^{0 \rightarrow s_f} \left(\mathbf{R}_{6 \times 6}^{0 \rightarrow s_i} \right)^{-1} \quad (1)$$

After algebraic manipulation, the momentum compaction function can be expressed in terms of Twiss parameters as

$$R_{s_6}(s_i \rightarrow s_f) = \left[\left(\frac{s_i - L_b}{\rho_b^2} \sqrt{\beta_i \beta_f} + \frac{s_i \alpha_i}{\rho_b^2} \sqrt{\frac{\beta_f}{\beta_i}} \right) \sin \psi_f + \left(\frac{s_i L_b}{\rho_b^2} \sqrt{\frac{\beta_f}{\beta_i}} \right) \cos \psi_f \right] s_f \quad (2)$$

where L_b and ρ_b are the dipole length and radius, α and β are Twiss parameters, and ψ is the betatron phase. The subscripts i and f are denoted respectively the locations at the exit of the first dipole and the entrance to the second one. In Eq. (2) we have made thin-dipole approximation and assumed the two dipoles are the same. The goal is to make Eq. (2) small throughout an isochronous beamline so that the CSR kernel is kept small [15] and thus microbunching gain development along the beamline is small.

By examining the parametric dependencies of the relative momentum compaction function (see Figs. 2 and 3), we propose a set of sufficient conditions to make it as small as possible throughout the beamline: “small β functions within dipoles [17]; avoidance of small α functions within dipoles; keeping the betatron phase differences between dipoles close to an integer multiple of π .” It can be shown that the above conditions can result in small or minimized transverse beam emittance [18]. A slight difference of the above conditions from those for minimizing CSR-induced emittance growth is that these conditions should be taken care of for every pair of dipoles, not just cell units. Notice that we limit ourselves here to the *special* case of dipole-achromat-dipole module. The observation that the proposed conditions work for *general* beamline lattices still appears heuristic; their connection and extension to more general cases of dispersive in-between section are underway.

* This material is based upon work supported by the U.S. Department of Energy, Office of Science, Office of Nuclear Physics under contract DE-AC05-06OR23177.
[#]jcysai@vt.edu

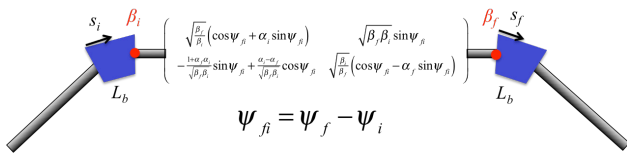
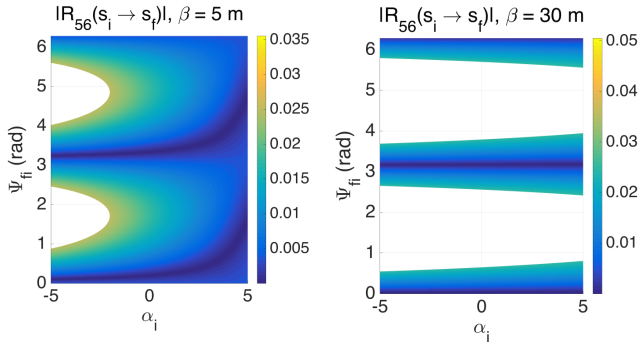
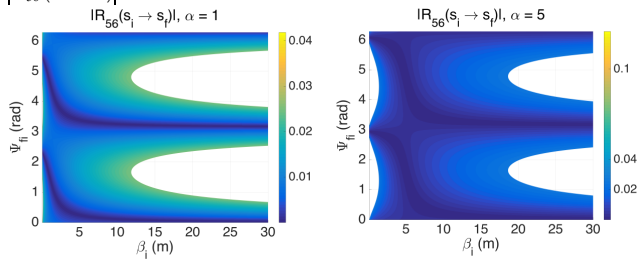


Figure 1: Illustration of [dipole-straight-dipole] beamline.

Figure 2: Relative momentum compaction as functions of Ψ_{fi} and α . In both figures the colored areas are for $|R_{56}(s' \rightarrow s)| \leq 0.025 \text{ m}$. Here assume $\rho = 10 \text{ m}$ and $L_b = 1 \text{ m}$.Figure 3: Relative momentum compaction as functions of Ψ_{fi} and β_i . In both figures the colored areas are for $|R_{56}(s' \rightarrow s)| \leq 0.025 \text{ m}$. Here assume $\rho = 10 \text{ m}$ and $L_b = 1 \text{ m}$.

EXAMPLES

Having proposed the conditions for suppression of CSR gain, in this section we would examine them, together with those for CSR-induced emittance minimization, in the following four example lattices. These four examples form two sets. The first set aims to demonstrate *both* the CSR emittance minimization (or cancellation) *and* CSR microbunching gain suppression are both achieved in one case and neither in the other. The second set is to illustrate the CSR microbunching is appreciable while CSR-induced emittance growth is still well preserved.

As for the first set of example lattices (hereafter denoted Example 1 and Example 2 lattices), they are two 1.3-GeV recirculation arcs, with the peak bunch current 65.5 A, normalized emittance $0.3 \mu\text{m}$, and uncorrelated energy spread 1.23×10^{-5} . Example 1 and 2 are both 180° arcs with locally larger momentum compaction R_{56} for Example 1 than Example 2. Further, Example 1 is globally isochronous while the isochronicity of Example 2 is local. Figure 4 shows the Twiss and momentum compaction functions across the arcs. The resultant CSR-induced emittance growths and microbunching gains for the two Examples are shown in Figs. 5 and 6, respectively. From Fig. 5 one can see the beam emittance

is well preserved in Example 2 while features four times increase for 500 pC in Example 1. From Fig. 6, one can see Example 1 is subject to CSR microbunching instability while Example 2 is not. These gain curves were obtained by our recently developed Vlasov solver [1] with benchmarking of the results against particle tracking by ELEGANT [19].

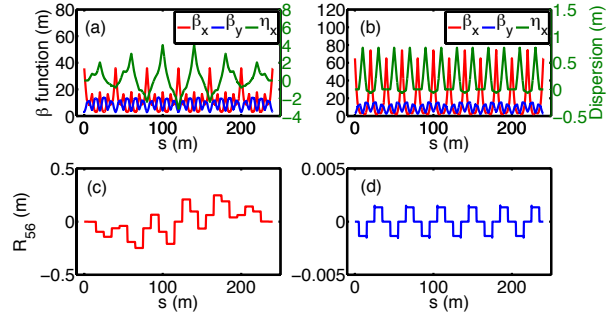
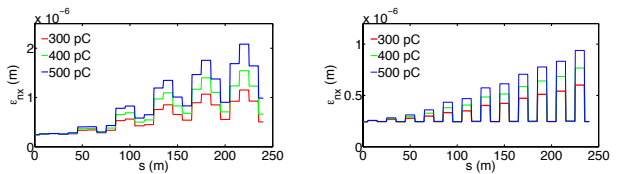
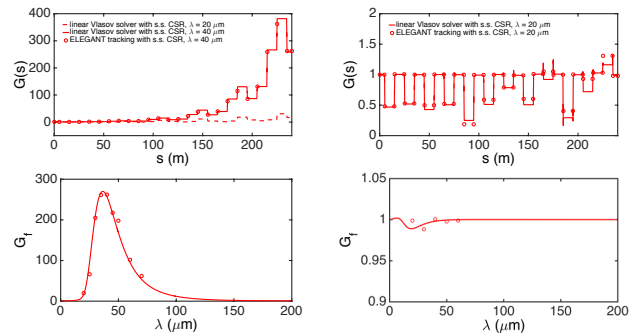
Figure 4: Twiss (top) and R_{56} (bottom) functions for Example 1 (left) and Example 2 (right) lattices. Note the scale difference between two bottom figures.

Figure 5: Evolution of the transverse normalized emittances for Example 1 (left) and Example 2 (right) lattices.

Figure 6: CSR microbunching gain functions for $\lambda = 20 \mu\text{m}$ and $40 \mu\text{m}$ (top) and gain spectra (bottom) for Example 1 (left) and Example 2 (right) lattices. Dots are benchmarking data from ELEGANT tracking [19].

Now we examine our proposed conditions for the two lattices. Figure 7 compares Twiss functions within dipoles and betatron phase differences between near-neighbor dipoles. One can see from the top row of Fig. 7 that α 's for Example 2 are in general larger than for Example 1. Moreover, the phase differences between neighboring dipoles for Example 2 ~ 0 or $\sim \pi$ also satisfy the emittance compensation [9]. In contrast, Example 1 does not follow; thus the emittance growth can be expected (see Fig. 5). From Fig. 7, Example 2 lattice meets our proposed conditions and thus has CSR gain suppressed.

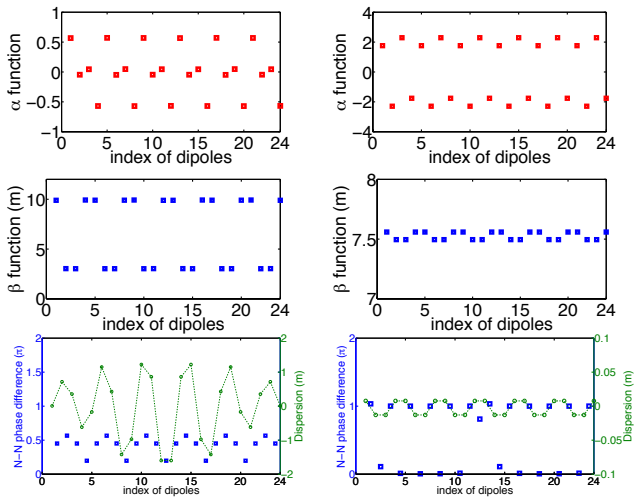


Figure 7: Twiss functions and betatron phases for Example 1 (left) and Example 2 (right) lattices. Here dots are the values taken from the center of each dipole.

For the second set of examples (Example 3 and Example 4 lattices), they are two medium-energy quasi-isochronous arcs. Example 3 [20] is based on the design of an example arc outlined in Ref. [7]. The entire arc is achromatic and quasi-isochronous. The Example 4 is similar to Example 2 but intended for lower beam energy 120 MeV. Suppression of CSR-induced emittance has been taken care for both examples. Figure 8 illustrates Twiss and the momentum compaction functions along the beamline, in which the momentum compactions for the two lattices can be different by an order of magnitude. Figures 9 and 10 show the CSR-induced emittance growths and microbunching gains, respectively. In Fig. 9, the beam emittances for Example 3 and 4 are largely preserved. From Fig. 10, one can see moderate CSR gains in Example 3 while nearly no gain amplification is observed for Example 4.

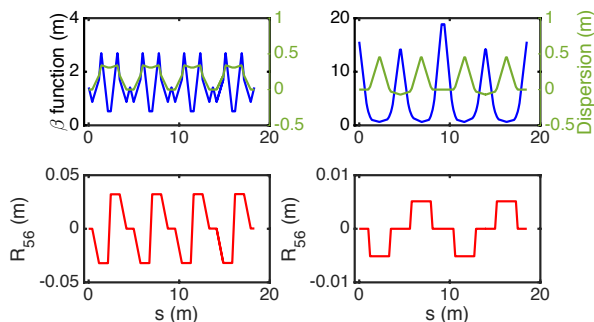


Figure 8: Twiss (top) and R_{56} (bottom) functions for Example 3 (left) and Example 4 (right) lattices.

Comparison of Twiss functions and betatron phases for Example 3 and Example 4 is shown in Fig. 11. Having examined our proposed conditions, we found the α functions for Example 3 are relatively smaller than those of Example 4. In the bottom row of Fig. 11, it is found the phase differences for both Example 3 and Example 4 satisfy the requirements outlined in Ref. [9]; thus guarantee the preservation of the beam emittances.

However, Example 4 is more preferred than Example 3 in view of our proposed CSR gain suppression conditions.

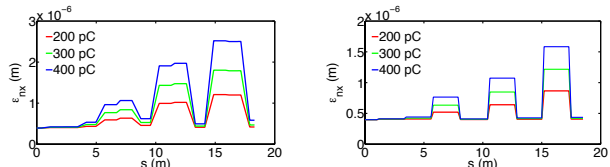


Figure 9: Evolution of the transverse normalized emittances for Example 3 (left) and Example 4 (right) lattices.

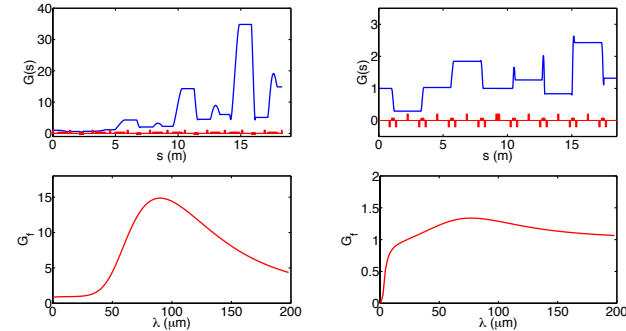


Figure 10: CSR microbunching gain functions with $\lambda = 90 \mu\text{m}$ (top) and gain spectra (bottom) for Example 3 (left) and Example 4 (right) lattices.

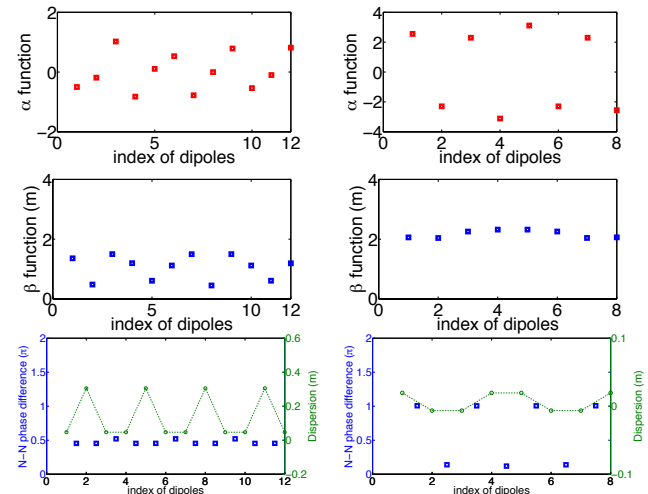


Figure 11: Twiss functions and betatron phase differences for Example 3 (left) and Example 4 (right) lattices. Here dots are the values taken from the center of each dipole.

CONCLUSION

In this paper we have overviewed the existing suppression schemes for CSR-induced emittance growth and microbunching gain enhancement. Based on our previous work [16], we have proposed a set of conditions for minimizing the kernel through the beamline design. These proposed conditions are sufficient; they do not exclude other possible cases. By illustrating the two sets of comparative examples, these conditions are examined and the optics impact on microbunching development is confirmed.

REFERENCES

- [1] C. -Y. Tsai *et al.*, Linear Vlasov Solver for Microbunching Gain Estimation with Inclusion of CSR, LSC and Linac Geometric Impedances, FEL'15 (MOP052)
- [2] D. Douglas, Suppression and enhancement of CSR-driven emittance degradation in the IR-FEL Driver, JLAB-TN-98-012, 1998
- [3] R. Hajima, A First-Order Matrix Approach to the Analysis of Electron Beam Emittance Growth Caused by Coherent Synchrotron Radiation, Japanese Journal of Applied Physics, 42 (2003)
- [4] S. Di Mitri *et al.*, Cancellation of Coherent Synchrotron Radiation Kicks with Optics Balance, Phys. Rev. Lett. 110, 014801 (2013)
- [5] Y. Jing *et al.*, Compensating effect of the coherent synchrotron radiation in bunch compressors, Phys. Rev. ST Accel. Beams 16, 060704 (2013)
- [6] C. Mitchell *et al.*, Longitudinal pulse shaping for the suppression of coherent synchrotron radiation-induced emittance growth, Phys. Rev. ST Accel. Beams 16, 060703 (2013)
- [7] D. Douglas *et al.*, Control of coherent synchrotron radiation and microbunching effects during transport of high brightness electron beams, arXiv: 1403.2318v1 [physics.acc-ph] and D. Douglas *et al.*, Control of synchrotron radiation effects during recirculation, IPAC'15 (TUPMA038)
- [8] Y. Jiao *et al.*, Generic conditions for suppressing the coherent synchrotron radiation induced emittance growth in a two-dipole achromat, Phys. Rev. ST Accel. Beams 17, 060701 (2014)
- [9] M. Venturini, CSR-induced emittance growth in achromats: Linear formalism revisited, NIM A 794 (2015), pp. 109-112
- [10] E. L. Saldin *et al.*, Longitudinal space charge-driven microbunching instability in the TESLA Test Facility linac, NIM A 528 (2004), pp. 355-359
- [11] Z. Huang *et al.*, Suppression of microbunching instability in the linac coherent light source, Phys. Rev. ST Accel. Beams 7, 074401 (2004)
- [12] C. Behrens *et al.*, Reversible electron beam heating for suppression of microbunching instabilities at free-electron lasers, Phys. Rev. ST Accel. Beams 15, 022802 (2012)
- [13] J. Qiang *et al.*, Suppression of Microbunching Instability Using Bending Magnets in Free-Electron-Laser Linacs, Phys. Rev. Lett. 111, 054801 (2013)
- [14] S. Di Mitri and S. Spampinati, Microbunching instability suppression via electron-magnetic-phase mixing, Phys. Rev. Lett. 112, 134802 (2014)
- [15] C. -Y. Tsai *et al.*, Conditions for CSR microbunching gain suppression (in preparation)
- [16] C. -Y. Tsai *et al.*, Multistage CSR microbunching gain development in transport or recirculation arcs, FEL'15 (MOP087)
- [17] Too small β function means very strong focusing, which can cause other issues. Beamline designers usually strike a balance among them.
- [18] A. Ropert, Low emittance lattices, CERN Accelerator School: 5th Advanced Accelerator Physics Course, Rhodes, Greece (1993)
- [19] C. -Y. Tsai and R. Li, Simulation of coherent synchrotron radiation induced microbunching gain using ELEGANT, JLAB-TN-14-016
- [20] S. Di Mitri, Intrabeam scattering in high brightness electron linacs, Phys. Rev. ST Accel. Beams 17, 074401 (2014)